The function of the spine and its morphological effect in quadruped robot locomotion

Zhao, Qian ; Sumioka, Hidenobu ; Yu, Xiaoxiang ; Nakajima, Kohei ; Wang, Zhimin ; Pfeifer, Rolf

DOI: https://doi.org/10.1109/ROBIO.2012.6490945

Proceedings of the 2012 IEEE
International Conference on Robotics and Biomimetics
December 11-14, 2012, Guangzhou, China

The Function of the Spine and its Morphological Effect in Quadruped Robot Locomotion

Qian Zhao, Hidenobu Sumioka, Xiaoxiang Yu, Kohei Nakajima, Zhimin Wang, and Rolf Pfeifer

Abstract— **In quadruped animals, spinal movements contribute to locomotion in terms of controlling body posture, providing the foundation to generate leg movement, and integrating limb and trunk actions. Inspired by this biological findings, we develop two quadruped models featuring different numbers of spinal joints to demonstrate the spine-driven locomotion behaviors. To gain a deep understanding of how the locomotion is achieved by axial driven propulsion and how the spinal morphology affects locomotion, we exclusively employ actuated spinal joint(s) to the model with a minimalistic control strategy. We choose three individuals from these two models and analyze their behaviors in terms of gait properties, i.e., angle of attack, ground clearance, and movement of the center of mass. The results show that employing the spinal morphology with two joints can greatly enhance the stability and speed of locomotion. Among several advantageous properties of the two spinal joint model we identify the following. First, it allows the robot to adjust the movement of the center of mass to stabilize itself. Second, by providing more freedom to bend the spine, the robot can pull the rear legs forward, thus increasing the stride length. Finally, locomotion with this model exhibits two flight phases and greater flight proportion during each stride, similar to what it is observed from running cheetahs, which make significant difference in the speed and the gait.**

I. Introduction

Legged robotics has drawn much more attention from robotic researchers due to its applications in rough terrains in nature and in our living environments [1]. Most of the existing quadruped robots are very similar in their morphology, and feature a single rigid body with four legs with individually actuated hips and/or knees. However, the resulting locomotion behavior is much more constrained than its natural counterpart in terms of speed, energy efficiency, maneuverability, and adaptivity to rough terrain.

From a biological point of view, one of the major differences between robots and animals is the spine. It is central to the control of body posture, provides the foundation to produce the leg's movement, and integrates limb and trunk actions [2]. Principally, quadruped animals use rhythmic movements of the body stem with its axial skeleton and legged locomotion strategies in parallel [3]. For example, a cheetah, the fastest animal in the land, is able to reach up to 110 km/h for a short dash. The main role of its spine is to make extensive body articulation, thus leading to greater power and speed.

Nevertheless, there have only been a few attempts to introduce a spine to a robotic platform, while substantial effort has been put on the design and optimization of leg's morphology and its associated controller [4], [5], [6]. Recently, some researchers have come to realize the important role the spine plays in locomotion, but most only focused on the controller of the spinal joint, and barely paid attention to its morphology [7], [8], [9]. All the aforementioned studies simply introduced a spinal joint connecting the fore and rear part without further study on its morphological parameters and anatomical structure, e.g., the position/number of the joints.

The concept of embodiment suggests that a system's behavior is generated through the interaction between controller, body (morphology) and environment [10]. A system even without a controller is able to generate versatile and meaningful behavior. For example, a new study has demonstrated how the arrangement of springs located in the spine generates and affects locomotion behavior of going down a slope without external energy in a passive quadruped robot [11]. If we look back to the anatomical structure of a biological spine, we find more important spinal morphological parameters need to be investigated further, except spinal stiffness, to gain a deep understanding of its underlying mechanism.

In this paper, we introduce two spinal morphologies differing in the number of spinal joints into a quadruped model to demonstrate the spine-driven locomotion behavior. Three individuals from these two spinal morphologies are selected and compared regarding the attack angle, the ground clearance (GC), and the movement of the center of mass (CoM). The simulation results show that the locomotion can be greatly enhanced by employing lumbosacral joint and thoracic joint together in terms of the stability and speed.

II. Design

In this section, we describe the design of the spinal morphologies and its associated models. Next, the selection of the morphological parameters and the design of controller are presented.

A. Spinal morphology design

The spine is made up of small bones, known as vertebrae, that are stacked on top of each other to create the spinal column. The number of vertebrae varies with the species of

This research was funded by the European Community's Seventh Framework Programme FP7-ICT-248311(AMARSi).

Q. Zhao, H. Sumioka, X.Yu, K. Nakajima, and R. Pfeifer are with Department of Informatics, University of Zurich, 8050, Zurich, Switzerland, email: zhao@ifi.uzh.ch.

H. Sumioka has moved to Advanced telecommunications research institute international, email: sumioka@atr.jp.

X. Yu is also with Bio-Inspired Robotics Lab, Swiss Federal Institute of Technology Zurich, 8092 Zurich, Switzerland.

Z. Wang is with Fudan University, China.

978-1-4673-2127-3/12/$31.00 © 2012 IEEE

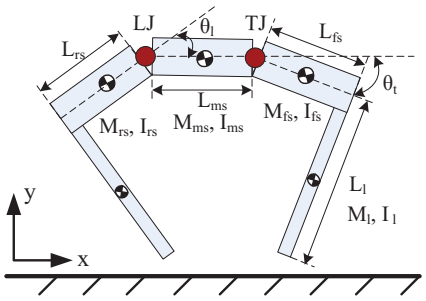

Fig. 1. Planar quadruped model of M2. Red dots stand for the actuated spinal joints. The specifications of the model are shown in Table I.

the animals from ten in frogs to fifty six in tigers. All of the spinal movements are distributed over the connecting joints of these vertebrae. So it is too complex to analyze the spine-driven locomotion by taking many joints into account.

We know that the spinal column consists of lumbosacral spine, thoracic spine, and cervical spine [12]. So we employed a spinal joint with one degree of freedom to emulate the movement of each part. Since the head's movement has less effect on locomotion, we ignored cervical spine in this paper. We employ a lumbosacral joint (LJ) to mimic the role of lumbosacral spine in locomotion. Similarly, the thoracic joint (TJ) is taken to emulate the function of thoracic spine.

As a starting point, we only applied LJ into the model to study the role of lumbosacral spine, because lumbosacral spine's main motions are bending and extending [13], which could greatly benefit locomotion. LJ is located in the rear part of the spine, inspired by the biological finding which suggests that the rear position of LJ can produce a particularly pronounced sagittal displacement of the pelvis [3]. We define the model with LJ as morphology one (M1). M1 consists of three segments which are a pair of stick-shaped legs, and a spine with a LJ. We simplified this model by taking out the leg actuation, to focus on the study of spine-driven locomotion and the effects of spinal morphology on locomotion.

Because of the existence of a small amount of flexion-extending movement in thoracic spine [14], we added a TJ in the middle between the shoulder and the LJ (Fig. 1) to investigate how it contributes locomotion, along with lumbosacral spine. The model with these two joints is named by morphology two (M2). If we fix the movement of TJ, which is θ_t in Fig. 1, and kept the rest parameters of M2, then M2 becomes M1.

We copied some of cheetah's morphological parameters (weights and sizes of the body and legs), and applied them to the models, because a cheetah exhibits noticeable spinal flexion and extension movement when running[15]. Table I details morphological parameters we have chosen for M2.

B. Controller design

1) Minimalistic control strategy: We employed a minimalistic control strategy to this model [16], in which the angular position of the spinal joints is determined by the sinusoidal curve as follows:

$$\theta_l(t) = A_l \sin(2\pi f_l t) + \psi_l \quad (1)$$

$$\theta_t(t) = A_t \sin(2\pi f_t t + \phi_t) + \psi_t \quad (2)$$

where θ_l and θ_t indicate the target angular positions of the motors controlling LJ and TJ, respectively. A, f and ψ designate the amplitude, the frequency, and the offset. The phase ϕ is the delay between the LJ and TJ. The subscript l and t denote LJ and TJ, respectively. By using this simple control scheme, we are able to evaluate how the morphological properties of the spine can contribute to locomotion behavior. The parameters used in the following experiments are heuristically determined as follows: $f_t = f_l = 1.5$, $A_l \in [17,33]$, and $\psi_l \in [-12,2]$. The rest control parameters (A_t, ψ_t, ϕ_t) will be optimized with genetic algorithm described in the following part. Time step t in this paper represents one actuation loop of the control program.

2) Genetic algorithm for the sinusoid function controller: The genetic algorithm (GA) is used to optimize the control parameters (A_t, ψ_t, ϕ_t) for TJ with the aim to achieve fast and stable locomotion behaviors. The population size is 60 while the number of generations is 10. The cost function is the speed multiplied by -1. The probabilities of crossover and mutation are 0.5 and 0.15, respectively. Each individual consists of three parameters which are encoded as three 8 bit genes. The boundaries of these three parameters are decided heuristically as follows: $A_t \in [15,25]$, $\psi_t \in [-4,4]$, and $\phi_t \in [-1.5708,-0.7854]$.

III. Simulation

In this section, the results of the overall exploration based on these two proposed models are presented first, followed by the selection of the best individual from M1, namely I1, and its comparison with the one from M2, namely I2. The latter has the same control parameters for the LJ as I1, to ensure fairness. Finally the best individual from M2, namely I3, is selected and analyzed in details.

A. Simulation Setup

We have implemented both models in Mathworks matlab 2009 (64bit), together with the SimMechanics toolbox.

In simulation, we constructed a physically realistic interaction model based on a biomechanical study [17]. The vertical ground reaction forces are modeled by one non-linear visco-elastic element, and the horizontal forces are calculated by

TABLE I

Morphological parameters for M2

Param.	Value	Param.	Value	Param.	Value
L_l	0.83 m	M_l	5 kg	I_l	0.29 kg· m^2
L_{rs}	0.33 m	M_{rs}	6.7 kg	I_{rs}	0.06 kg· m^2
L_{ms}	0.33 m	M_{ms}	6.7 kg	I_{ms}	0.06 kg· m^2
L_{fs}	0.33 m	M_{fs}	6.7 kg	I_{fs}	0.06 kg· m^2

L: length; M: weight; I: inertia.
l: leg; rs: rear spinal segment; ms: middle spinal segment; fs: fore spinal segment.

a sliding-stiction model. It switches from stiction to sliding when the velocity of the foot exceeds the specified threshold. We used 0.7, 0.8, and 0.01 m/s for the sliding, stiction friction coefficients and the threshold velocity, respectively. Simulations were started from an initial condition with a height of 0.1 m from a stationary state and run for 50 s.

B. Overall exploration based on two spinal morphologies

To achieve comprehensive behavioral analysis, we investigated the influence of amplitude (A_l) and offset (ψ_l) on the locomotion behavior. We varied A_l from 17° to 33°, and ψ_l from $-12°$ to 4° with the increment of 2° in M1. Then we keep the same control parameters for the LJ and optimize the rest three (A_t, ψ_t, ϕ_t) for the TJ in M2. These parameters, A_l and ψ_l significantly change the locomotion behavior: the robot exhibits a stable rapid locomotion; it runs slowly; it exhibits unstable behavior; or it falls over. In this paper, we use two methods together, the step-to-fall method and the apex return map, to judge the system's stabilizing behavior [18]. If the robot does not fall within 50 s and the error of two adjacent apex heights of the CoM is less than 0.15 m after initial transient, this run is considered to be successful and therefore the speed is recorded, otherwise it is a failure and the speed is set to 0 m/s.

Fig. 2 (a), (b) suggest that the locomotion is able to be generated by the spinal flexion and extension. M2 can move much faster than M1, and its best performance attains 2.3 m/s, while the best one from M1 is 0.63 m/s.

The attack angle is defined as the angle formed between the leg and the ground in the forward direction when the feet touch on the ground. In both morphologies, greater attack angle of rear legs (Fig. 2 (c), (d)) corresponds to faster speed (Fig. 2 (a), (b)). With a larger attack angle, the rear legs can rotate the robot's body around the contact point and push it more forward.

In the biological perspective, the CoM moves forward and backward alternatively with respect to its nose during locomotion [19]. We define the CoM_S as the distance between the position of CoM and the position of the robot's shoulder, instead of the nose. The range of the CoM_S gets wider, as a result of the increasing amplitude of the bending and extension movement (Fig. 2 (e), (f)). Wider range of the CoM_S (Fig. 2 (e), (f)) is associated with better performance (Fig. 2 (a), (b)), because it offers more freedom to adjust the CoM, benefiting the stabilization of the posture and the enhancement of the speed. Furthermore, with the increase of the speed in M1 and M2 (Fig. 2 (a), (b)), the values of the rear and fore boundaries of the CoM_S get smaller (Fig. 2 (g)-(j)), which means that the horizontal excursion of the CoM moves further to the anterior trunk region.

The function of GC is to overcome the obstacles. Higher GC (Fig. 2 (k)-(l)) corresponds to fast speed (Fig. 2 (a)-(b)). However, higher GC makes the robot unstable. It is easier to fall when the spinal movement is pronounced in M1, compared to M2. M2 is able to use an additional spinal joint (TJ) to reduce GC of fore legs, adjust the CoM, and stabilize the robot.

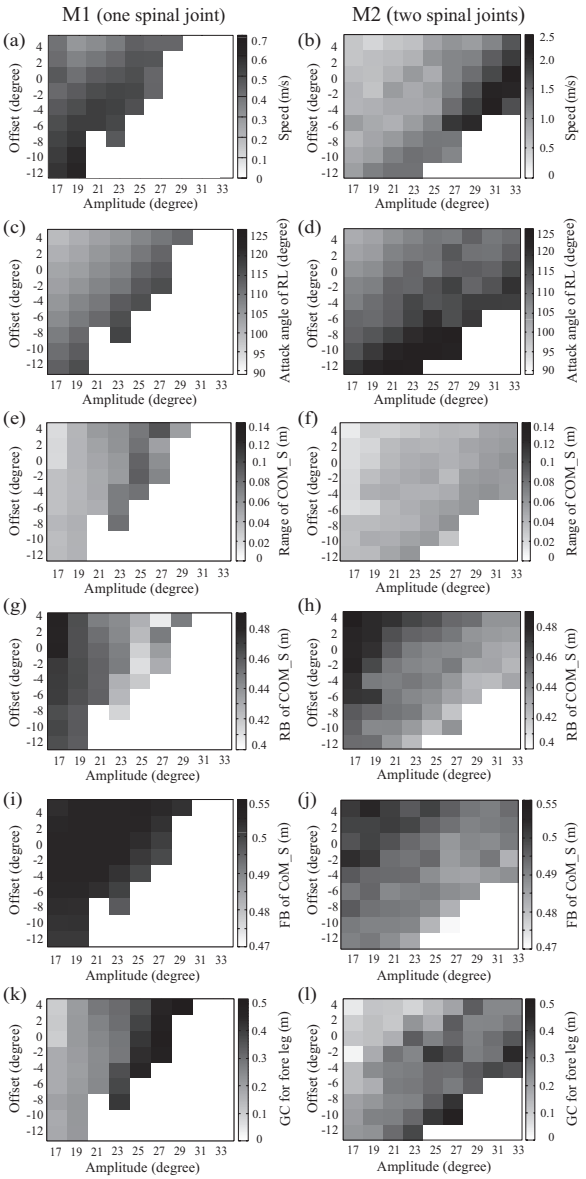

Fig. 2. Comparison results of two spinal morphologies (M1 in the left column and M2 in the right column). X axis is amplitude (A_l), and y axis denotes offset (ψ_l) for the LJ. The intensity of the cell represents the speed in (a), (b); the attack angle of real legs (RL) in (c), (d); the range of CoM_S in (e), (f); the rear boundary (RB) of CoM_S in (g), (h); the fore boundary (FB) of CoM_S in (i), (j); the ground clearance of fore legs (k), (l).

C. Basic effects of thoracic joint

To deeply compare the resulting behaviors from M1 and M2, we analyzed the behavior of I1 from M1, which attains 0.63 m/s (Fig. 3 (d)), and I2 from M2, which attains 1.25 m/s, defined previously (Fig. 3 (e)). Parameters obtained from the genetic algorithm described in the previous section are given in Table II.

1) Analysis on spine-driven locomotion: Fig. 4 (a), (b) show that the stable locomotion behavior of I1 and I2 can be achieved, even if leg actuation is not taken into account. We observe that four phases exist in I1 (Fig. 3(g)). Since the

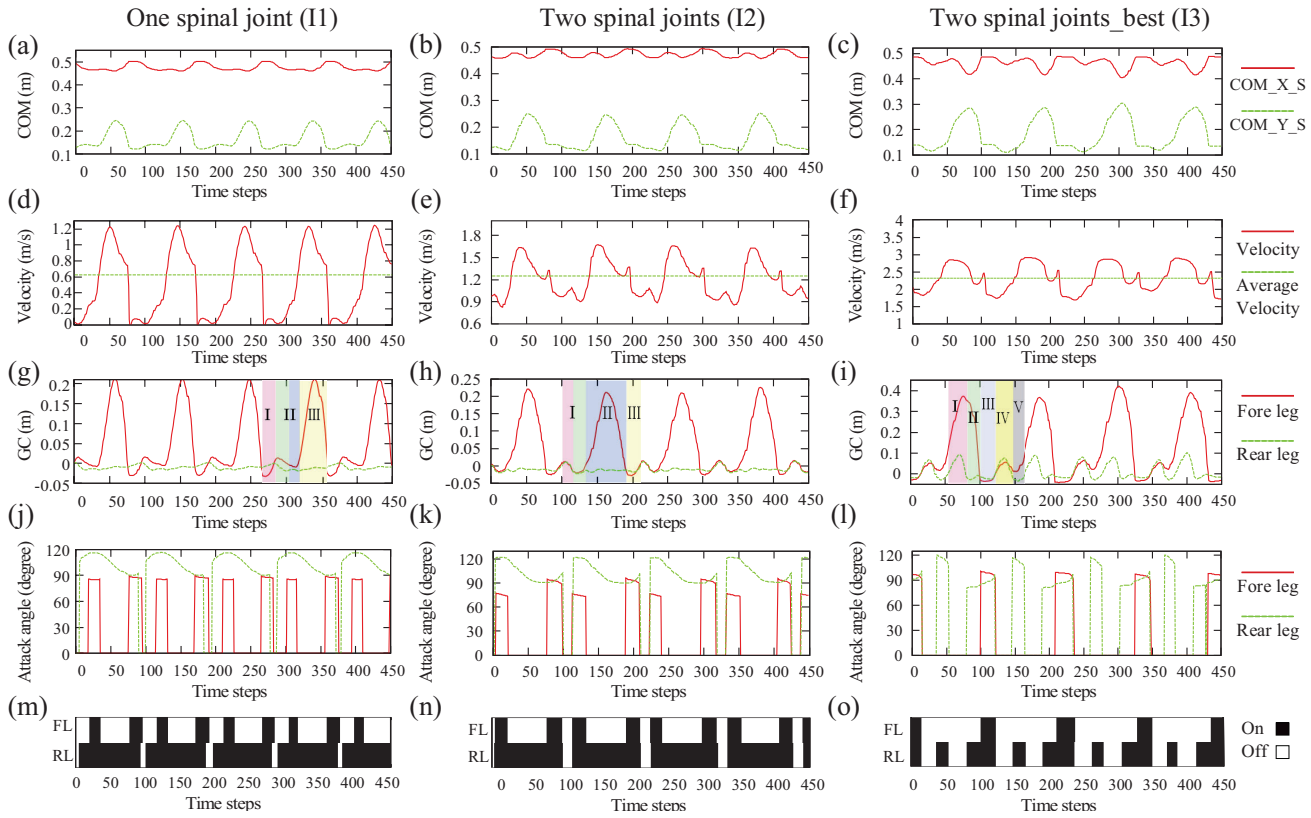

Fig. 3. The left, middle, right column are the results of I1, I2, and I3, respectively. The x axis represents time steps. The y axis stands for the movement of CoM relative to the shoulder (a), (b), (c); the velocity (c), (d), (e); the height of ground clearance (g), (h), (i); and the attack angle (j), (k), (l). In (g), (h), (i), areas shaded stand for phases, consistent with phases marked in Fig. 4. The footfall patterns of I1, I2, I3, are represented in (m), (n), and (o).

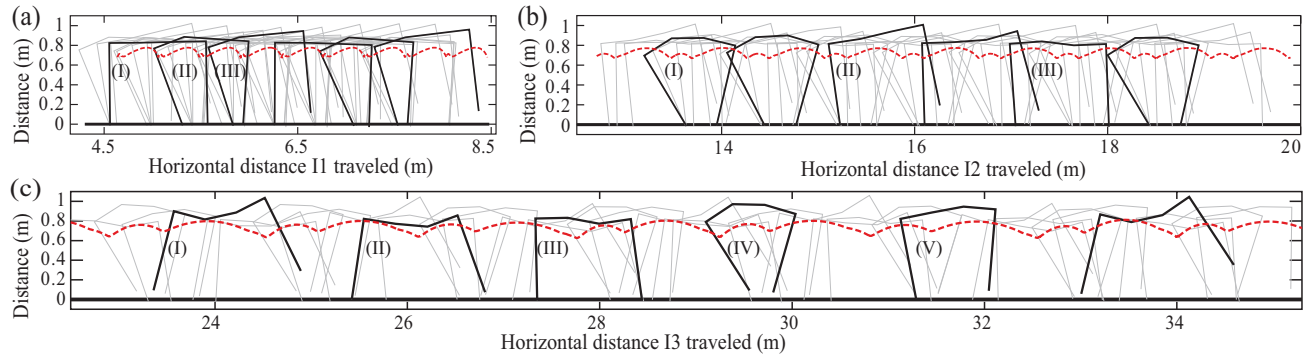

Fig. 4. Stick figures illustrating three different behaviors in simulation. The body postures are illustrated every 94 and 658 (94×7) simulation steps (a), and every 105 and 630 (105×6) simulation steps (b), (c) (gray and black stick figures, respectively). Red dotted line represent the trajectories of absolute CoM. (a) I1 ($A_l = 19°$, $\psi_l = -12°$). (b) I2 ($A_l = 19°$, $\psi_l = -12°$). (c) I3 ($A_l = 31°$, $\psi_l = -4°$).

phase shaded by green has very short duration, low GC of fore legs with 0.016 m , and almost has the same posture as the one after it shaded by blue, we assign both to phase II. I1 is featured with three prominent phases as shown in Fig. 4(a). Starting from the original posture (phase I), the spine is flexed and the rear legs are pulled forward until the maximum (phase II). This moves the CoM forward. Afterwards, the spine is extended to allow the lift up of the fore legs, leading to the back-moving of the CoM (phase III). In the next step, the fore legs touch the ground, and the CoM moves forward again (back to phase I). The same process repeats.

Similarly as I1, I2 also has three important phases (4 (b)). The difference with I1 comes from the further flexed spine caused by combining the flexion of LJ and TJ. This then pulls the rear legs more forward than I1 (phase I) and leads to a higher attack angle of 123° (Fig. 3(l)), compared to I1 with 116° (Fig. 3(j)). The rest of the cycle follows the same procedure as in I1.

2) Ground clearance: GC for the fore legs is almost the same in I1 and I2. It has two peaks: one lower about 0.015

m, and the other one higher about 0.22 m. However, GC for the rear legs is different for I1 and I2. The former has its GC barely noticeable (0.003 m), while the latter has a much higher GC (0.01 m). This is due to the inclusion of the flexion of the additional spinal joint (TJ).

3) Attack angle: In these two spine-driven models, attack angle is changed along with the body posture controlled by the spinal controller.

Wider range of attack angle of fore legs in I2 enhances locomotion, because it is able to increase the stride length by propelling the body forward further. It varies from 94° to 74° in phase I (Fig.3 (k)), as a result of the additional flexion of TJ. Therefore, it can push the body forward further than I1, whose angle is almost constant, 90° (Fig.3 (j)). In addition, larger attack angle of rear legs contributes to the increase of the stride length by pushing the body more forward.

4) Movement of the center of mass: Fig. 3 (a), (b) show that the horizontal motion of the CoM in the body is only determined by flexion and extension of the back. This underlines the determinant role of the spine as the main engine for the locomotion.

The movement of CoM relative to the shoulder is not constant (Fig. 3 (a), (b)). The horizontal excursion of the CoM is in coupling with the motion of the spine. During spinal extension, the CoM moves to the posterior part of the spine, but it moves to the anterior part during spinal flexion. This horizontal excursion equals about 4%, 4% of the model's length in I1, I2, respectively. The extension phase of the spine is coupled with a upward movement of the CoM. In the flexion phase, after initial ascent, the CoM moves downward (Fig. 3 (a), (b)). The excursion of the vertical movement of the CoM is about 14%, 16% of the model's length in I1, I2, respectively.

D. Dynamic locomotion induced by double flight phase

To know how well M2 is able to perform, we pick the fastest one from M2, namely I3, and compare it with I1 and I2. I3 can reach up to 2.3 m/s (Fig. 3 (f)) .

1) Analysis on spine-driven locomotion: There is a high degree of co-ordination between spinal flexion and the placing of the feet on the ground to maximize stride and increase speed in I3. I3 mainly differs from I1 and I2 in the gait. It is characterized by five phases, two of which are flight phases, instead of one, in each stride, as shown in Fig. 3 (i). Fig. 4 (c) shows that one takes place when the spine is at maximum extension (phase I); the other one happens when sharp contraction of the spine takes place before the rear feet contact the ground (phase IV). The period of one cycle of I3 is the same as I2 and longer than I1, but speed is much faster than both. The double flight phases can account for its fast speed.

2) Ground clearance: I3 has pronounced GC not only for fore legs with 0.37 m, but for rear legs (Fig. 3 (i)) . It exhibits two flight phases in rear legs in each cycle: one is with GC of 0.073 m and the other one is of 0.09 m, which are much larger than I1 and I2.

3) Attack angle: For the rear legs, it has similar value of attack angle to I2, but it has a a smaller lift up angle of 80°, which can crouch more and push the body forward further, compared to I2 with the angle of 90°.

4) Movement of the center of mass: Fig. 3 (a), (b), (c) show that I3 has similar horizontal and vertical movement of the CoM to I1 and I2 during one cycle. This horizontal excursion equals around 6% and vertical excursion is about 20% of the model's length in I3.

Table. III shows the boundaries and the range of the CoM_S in horizontal and vertical direction. We observed that values of fore boundary and rear boundary of the horizontal movement of CoM_S in I2 and I3 are smaller than I1, which suggests that I2 and I3 are able to move the CoM forward more efficiently than I1, benefiting the rapid locomotion. Moreover, the excursion range of the CoM_S in I2 and I3 is wider than I1, offering more freedom to adjust the CoM to stabilize the robot itself.

IV. Discussion

I2 is capable of producing more pronounced spinal movements, which contribute to the increase of the stride length by pulling the rear legs forward further than I1, thus increasing the stride length. The attack angle of fore legs of I2 (73°) is less than I1 (85°) when they lift off the ground, caused by additional TJ, which can propel the body forward. We believe that multiple spinal joints are able to provide the body with more freedom to enlarge the swing of the limbs and increase the stride length.

I2 and I3 mainly differ in the speed and the gait, as a result of the amplitude of spinal movements (Table. II). I3 almost runs twice as fast as I2. It reaches the maximal extension and flexion in two flight periods per stride, while I2 is only suspended once in each stride. In addition, the gait of I3 exhibits greater proportion of flight in total stride. These results are consistent with studies of the motions of the running cheetah and horse [15]. A horse, with relatively rigid spine generating less spinal movements, can be represented by I2, and a cheetch, featuring pronounced spinal movements, is suitable to be simplified as I3. We conclude that the double flight periods, together with greater proportion of flight, contribute to its longer stride [15]. However, I3 exhibits a double stance

TABLE II
PARAMETERS FOR I1, I2 AND I3

	A_l	ψ_l	A_t	ψ_t	ϕ_t
I1	19°	−12°	/	/	/
I2	19°	−12°	16.4°	−3.2°	-0.9
I3	31°	−4°	23.8°	3°	-0.9

TABLE III
RESULTS OF CoM_S IN I1, I2, I3

	CoM_$S_{horizontal}$ (m)			CoM_$S_{vertical}$ (m)		
	$Fore_b$	$Rear_b$	Range	Low_b	$High_b$	Range
I1	0.46	0.5	0.04	0.25	0.12	0.13
I2	0.45	0.49	0.04	0.25	0.12	0.14
I3	0.42	0.48	0.06	0.29	0.11	0.18

phase (phase III in Fig. 4 (c)), which does not exist in cheetah running. We could eliminate this phase by adding actuated hip joints. When the rear feet touch on the ground in phase II, the rear hip motor is actuated and the leg is swung outward. As a consequence, the body is propelled forward and the rear feet are off the ground in the next phase, which might avoid the presence of this double stance phase.

The horizontal excursion of CoM relative to shoulder equals about 4%, 4%, 6% of the model's length in I1, I2, I3, respectively. They are less than 15% from pika [19], which could be improved by introducing more spinal joints. The spinal joint in this sense can be defined as the connecting point of vertebrae in animals. A cat has thirty vertebrae in its spinal column, five more vertebrae than a human. This might account for its spine's agility and rapid speed.

The amplitude of the vertical motion relative to the nose is about 14%, 16%, 20% of the model's length in I1, I2, I3, respectively. This is higher than the the average value of 10 % observed from human [20] and pika [19] running. The reduction of the vertical displacement of the CoM could be achieved by introducing springs in the legs and adjusting their spring-mass systems by increasing the angle swept by the stance legs while keeping leg stiffness nearly constant [21] [22].

V. Conclusion and Outlook

This novel study suggested that the motion of the spine is a determinant factor in the locomotion. The change of spine posture serves the placement of the CoM relative to the ground contact point, working as an engine to propel the body; limbs might be looked at as servants of the trunk to assist locomotion [12].

M2 performs better than M1 in terms of the speed and stability. M2 is able to produce more freedom to pull the rear legs forward, increase the stride length, and move the CoM more efficiently forward. Therefore the speed is increased. In addition, it benefits stability by using additional TJ to optimize the movement generated by the LJ by readjusting unstable posture or enhancing the extension-flexion movement. I3, the best individual from M2, outperforms I2 due to its double flight phases and greater proportion of flight in total stride, as a result of more pronounced spinal movement. This is similar to what we observe from the cheetah's running, which makes significant difference in the speed and gait.

In the future, compliant and actuated legs will be introduced to study how to reduce vertical excursion of the CoM. In addition, the way of how to coordinate legs' movement and the spine's movement would be another direction.

References

[1] R. M. Alexander, *Principles of Animal Locomotion*. Princeton University Press, 2002.

[2] S. N and C. DR, "Function of the epaxial muscles in walking, trotting and galloping dogs: implications for the evolution of epaxial muscle function in tetrapods," *J Exp Biol*, pp. 1490–1502, 2010.

[3] M. S. Fischer and H. Witte, "Legs evolved only at the end," *Phil. Trans. R. Soc. A*, vol. 365, no. 1850, pp. 185–198, 2007.

[4] I. Poulakakis, J. A. Smith, and M. Buehler, "Modeling and experiments of untethered quadrupedal running with a bounding gait: The Scout II robot," *Int. J. Rob. Res.*, vol. 24, pp. 239–256, April 2005.

[5] S. Rutishauser, A. Sproewitz, L. Righetti, and A. J. Ijspeert, "Passive compliant quadruped robot using central pattern generators for locomotion control," in *2008 IEEE International Conference on Biomedical Robotics and Biomechatronics*, 2008.

[6] K. Byl, A. Shkolnik, S. Prentice, N. Roy, and R. Tedrake, "Reliable dynamic motions for a stiff quadruped," in *Experimental Robotics*, ser. Springer Tracts in Advanced Robotics, O. Khatib, V. Kumar, and G. Pappas, Eds. Springer Berlin / Heidelberg, 2009, vol. 54, pp. 319–328.

[7] M. A. Lewis and G. A. Bekey, "Gait adaptation in a quadruped robot," *Autonomous Robots*, vol. 12, pp. 301–312, 2002.

[8] K. F. Leeser, "Locomtotion experiments on a planar quadruped robot with articulated back spine," Master's thesis, Massachusetts Institute of Technology, 1996.

[9] U. Culha and U. Saranli, "Quadrupedal bounding with an actuated spinal joint," in *2011 IEEE International Conference on Robotics and Automation (ICRA)*, May 2011, pp. 1392–1397.

[10] R. Pfeifer and J. Bongard, *How the Body Shapes the Way We Think: A New View of Intelligence*. The MIT Press, 2006.

[11] M. H. H. Kani, M. Derafshian, H. J. Bidgoly, and M. N. Ahmadabadi, "Effect of flexible spine on stability of a passive quadruped robot: Experimental results," in *2011 IEEE International Conference on Robotics and Biomimetics (Robio)*, Dec. 2011, pp. 2793–2797.

[12] S. Gracovetsky, *The Spinal Engine*. Springer, cop, 1989.

[13] Billy, "Spinal coord injury resource center," 2012. [Online]. Available: http://www.spinalinjury.net/index.html

[14] L. Warnecke, "The stem of aplombcpart two: The thoracic spine," 2012. [Online]. Available: http://danceadvantage.net/2011/03/09/thoracic-spine/

[15] M. Hildebrand, "Motions of the running cheetah and horse," *journal of the Royal Society Interface the Royal Society*, vol. 40, no. 4, pp. 481–495, 1959.

[16] F. Iida and R. Pfeifer, "Sensing through body dynamics," *Robotics and Autonomous Systems*, vol. 54, no. 8, pp. 631–640, 2006.

[17] K. G. Gerritsen, A. J. van den Bogert, and B. M. Nigg, "Direct dynamics simulation of the impact phase in heel-toe running," *Journal of biomechanics*, vol. 28, no. 6, pp. 661–668, 1995.

[18] J. Rummel and A. Seyfarth, "Stable running with segmented legs," *Int. J. Rob. Res.*, vol. 27, no. 8, pp. 919–934, Aug. 2008.

[19] R. Hackert, H. Witte, and M. S. Fischer, "Interactions between motions of the trunk and the angle of attack of the forelimbs in synchronous gaits of the pika (ochotona rufescens)," in *Adaptive Motion of Animals and Machines*, 2006, pp. 69–77.

[20] C. R. Lee and C. T. Farley, "Determinants of the center of mass trajectory in human walking and running," *J Exp Biol*, pp. 2935–2944, 1998.

[21] F. CT, G. J, and M. TA., "Running springs: speed and animal size," *J Exp Biol*, no. 185, pp. 71–86, 1993.

[22] J. P. He, R. Kram, and T. A. McMahon, "Mechanics of running under simulated low gravity," *Journal of Applied Physiology*, vol. 71, no. 3, pp. 863–870, 1991.